Electro-Optic Sensor for Specific Absorption Rate Measurements

Sébastien Euphrasie[1], Shuo Zhang[1], Romain Butet[2], and Pascal Vairac[1]
[1]FEMTO-ST, Université de Franche-Comté, CNRS, ENSMM, UTBM, 25044, Besançon, France
[2]SATIMO, 225 rue Pierre Rivoalon, 29200, Brest, France

We propose a sensor system to measure the specific absorption rate at radio frequencies, using a matrix of electro-optic (EO) sensors. The aim is to replace the conventional metallic antenna scanned by a robot inside an open phantom with a matrix of small probes positioned inside a closed phantom. Results are presented for a dual sensor, showing the feasibility of the proposed approach. The two EO probes interrogated by the same laser are shown to detect electric fields smaller than 1 V/m. Measurements are conducted both with the probes in air and inside the phantom liquid.

In order to limit the risks associated with the use of mobile phones, the International Commission on Non-Ionizing Radiation Protection (ICNIRP) issued recommendations[1]. The Specific Absorption Rate (SAR) represents the electromagnetic (EM) power absorbed by a body by mass unit. It is defined by:

$$SAR = \sigma |E|^2 / \rho, \quad (1)$$

with σ and ρ the conductivity and density of human tissues, and E the rms electric field. The SAR is limited to 1.6 W/kg for 1 g of tissue in the United States[2] and to 2 W/kg for 10 g of tissue in Europe[3]. For practical purposes, the SAR of mobile phones is measured in a phantom filled with a normalized liquid by an isotropic EM sensor moved by a robot according to a normalized procedure[4]. This sensor consists of three orthogonal electrically short dipole antennas[5]. For each dipole, a low-threshold diode produces a DC output voltage proportional to the square of the electric field strength. Highly resistive - and therefore radio frequency (RF) transparent - lines act as low-pass filters and transmit the measurement information. With this kind of sensor, all frequency information is lost.

This method to qualify a mobile phone takes time, since the sensor has to scan the phantom and the liquid must be periodically recalibrated because of evaporation. To solve these issues, a matrix of static EM sensors can replace the robot. Using a matrix of metallic antennas may, however, greatly disturb the EM field and bias measurements. Electro-Optic (EO) probes can be used to overcome this problem. Each probe is sensitive to the electric field along only one direction. To have all information necessary to reconstruct the electric field inside the phantom, probes must then be oriented along three different directions.

Over the past two decades, EO crystals have been increasingly studied and used in order to measure EM waves[6-13]. Since they are completely dielectric, EO probes disturb EM fields far less than conventional metallic antennas. This advantage is crucial when using an array of sensors. Moreover, EO crystals such as lithium tantalate - $LiTa0_3$ - possess high relative permittivity ($\varepsilon_{ro} = 41$ for the ordinary axis and $\varepsilon_{re} = 43$ for the extraordinary in the case of $LiTa0_3$[7]), not far from the permittivity of the phantom liquid (41.5 at 900 MHz and 40 at 1.8 GHz), leading to even less disturbance. Furthermore, optical transport of information does not perturb and is not perturbed by the EM waves to be measured. Another advantage is the possibility to detect waves with frequencies from DC up to the Terahertz[6], since the EO effect works for this whole frequency range. The limiting factor for the upper frequency is the travel time of the optical beam trough the crystal, particularly in the case of techniques using multiple reflections. Finally, the probes can be miniaturized. The crystal volume can be made less than a millimeter cube, since minimum lateral dimensions are determined by the size of the laser beam. The thickness is linked to the sensitivity, but can be less than 1 mm for SAR applications[10].

Since the electric fields to be measured are weak (typically a few tens of volts per meter), the Kerr effect (quadratic EO effect) is negligible compared to the Pockels effect (linear EO effect). The Pockels effect is a non-linear optical effect which leads to a linear relation between the low-frequency electric field E and the second order impermeability tensor **η** at optical frequencies[14]:

$$\eta_{ij}(\vec{E}) = \eta_{ij}(\vec{0}) + r_{ijk} \cdot E_k \,, \tag{2}$$

with **r** the tensor of EO coefficients.

$$\overline{\overline{\eta}} = \varepsilon_0 \, \overline{\overline{\varepsilon}}^{-1} \,. \tag{3}$$

The result of this interaction leads to a small modification in the refractive indexes of the EO crystal and therefore to a change in the phase, the amplitude and the polarization state of a light beam passing through it. For instance, an electric field of 1 V/m along the extraordinary axis of a crystal of $LiTa0_3$ will lead to a variation of the extraordinary index $\Delta n_e = 1.7\ 10^{-10}$ (see equation (6) and Table 1).

There are several possible techniques to convert the modulation of the light beam into a change in intensity measured by a photodetector (see Refs. 7-8 for a good overview). For instance, a light beam with linear polarization along one optical axis of the EO crystal has its travel time modified by the electric field, according to the change in refractive index. Using a Mach-Zehnder interferometer with the EO crystal inserted in one arm converts the information about the electric field into a variation of intensity. However, the need to have two separate arms can limit the miniaturization of the probe.

Many EO sensors use a modification of the polarization of the light beam. The initial polarization is usually circular (but it can also be linear in some cases) and can be interpreted as two beams linearly polarized along two optical axes. Since the electric field impacts differently the two refractive indices, the induced phase retardation changes the overall polarization. Polarizers can then convert it into intensity variations. This technique is interesting since with a good choice of the EO crystal, including its cut, the probe can either detect a longitudinal or a transverse electric field. Each probe would need an optical element such as a quarter wave plate[12] or a Faraday rotator[11], however, which complicates the miniaturization and increases the total cost.

Another method of detection employs a Fabry-Perot resonant cavity. The light beam is polarized linearly along an optical axis. The change in the refractive index modifies the optical length of the cavity, and then the transmitted and reflected power. Sensitivity is proportional to the slope of the reflectance curve as a function of the optical path. Therefore, at the resonant wavelength of the cavity, this technique offers a very good sensitivity. However, for the case of several probes using the same laser beam, and therefore the same wavelength, it means that the thickness of all EO crystals must be nearly the same, which can be quite difficult to obtain in practice.

Designing a matrix of probes using a single laser for readout, we decided to adapt the last technique by reducing the efficiency of the dielectric mirrors. The sensitivities of the probes are correspondingly reduced but the thickness of the EO crystals is far less critical in this case.

In this letter, we present our experimental set-up and give the principle of our probes. We then show experimental results with both probes in air and inside the phantom liquid.

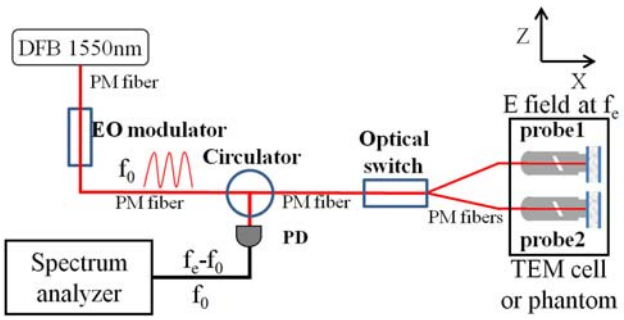

FIG. 1. Experimental set-up.

Our experimental set-up is depicted in Figure 1. It was designed to test the feasibility of measuring the electric field for SAR application with a matrix of EO sensors using a single laser. For the sake of demonstration, there are only 2 probes. To avoid absorption and diffusion inside the phantom liquid, the set-up is completely fibered with Polarization-Maintaining (PM) fibers. The laser source is a distributed feedback (DFB) laser diode operating around 1550 nm. Its output light is intensity-modulated at frequency f_0 (755 MHz in our case) by a commercial EO modulator, goes through a circulator, an optical switch, and then one of the two EO probes to go back to the circulator, and finally to a photodiode (PD) connected to a spectrum analyzer. There are two main advantages to using heterodyning. First, it limits perturbations coming directly from the antenna through EM compatibility. Second, it lowers the frequency the PD has to detect. The signal proportional to reflectance is at frequency f_0 and the signal proportional to the electric field is at frequency (f_e-f_0), f_e being the frequency of the field (typically 900 MHz or 1.8 GHz in our case). With such a system, no fast PD is required. Another possibility would have been to use a femtosecond laser[10]. The repetition of the short pulses would lead to the signal being modulated by a comb with a cardinal sinus shape. However, this kind of laser is rather expensive and their wavelength is hard to control precisely which could be problematic for practical applications.

The probes are made of 500 µm thick X-cut $LiTaO_3$ crystals. Since we only wanted to test the feasibility of the method, their lateral dimensions are 5 mm x 5 mm which is quite large but could be easily reduced to 1 mm or less, since the size of the laser beam determines the minimal lateral dimension of the crystals. The top (fiber end) and bottom (free end) surfaces were respectively covered with reflective coatings with reflection coefficients $R_1 = \rho_1^2 = 42\%$ and $R_2 = 92\%$. EO crystals are mounted on optical collimators terminated with a graded index lens. The laser beam is linearly polarized along the Z axis (extraordinary optical axis). As

explained in the following section, the probes are thus sensitive only to electric field parallel to the Z axis through the EO coefficient r_{33}. We preferred $LiTaO_3$ over $LiNb0_3$ because of its larger r_{33} coefficient and because its microwave dielectric constants (ε_{r0} and ε_{re}) are nearer to those of the liquid (cf. Table 1).

The probes were first tested in air, with the electric field generated by a TEM (Transverse EM) cell at a frequency f_e = 900 MHz[15]. According to finite elements simulations conducted with the commercial software CST Microwave, the amplitude of the electric field inside the EO crystals was 5 V/m. Subsequent measurements were conducted with stronger EM fields at 1.8 GHz, in air inside a waveguide and inside a phantom filled with its normalized liquid.

With a 3m uniaxial crystal such as lithium tantalate ($LiTa0_3$) or lithium niobate ($LiNb0_3$), the impermeability tensor is

$$\bar{\bar{\eta}}(\vec{E}) = \begin{pmatrix} \frac{1}{n_0^2} & 0 & 0 \\ 0 & \frac{1}{n_0^2} & 0 \\ 0 & 0 & \frac{1}{n_e^2} \end{pmatrix} + \begin{pmatrix} 0 & -r_{22} & r_{13} \\ 0 & r_{22} & r_{13} \\ 0 & 0 & r_{33} \\ 0 & r_{51} & 0 \\ r_{51} & 0 & 0 \\ -r_{22} & 0 & 0 \end{pmatrix} \begin{pmatrix} E_x \\ E_y \\ E_z \end{pmatrix}, \tag{4}$$

$$\bar{\bar{\eta}} = \begin{pmatrix} \frac{1}{n_0^2} - r_{22}E_y + r_{13}E_z & -r_{22}E_x & r_{51}E_x \\ -r_{22}E_x & \frac{1}{n_0^2} + r_{22}E_y + r_{13}E_z & r_{51}E_y \\ r_{51}E_x & r_{51}E_y & \frac{1}{n_e^2} + r_{33}E_z \end{pmatrix}, \tag{5}$$

with n_0 the ordinary and n_e the extraordinary refractive indices, and using the classical contraction of indices for tensor **r**. The EO coefficients, the refractive indices and microwave dielectric constants are given in Table 1 for $LiTa0_3$ and $LiNb0_3$[7].

TABLE I. **EO COEFFICIENTS, REFRACTIVE INDEXES AND DIELECTRIC CONSTANTS OF $LiTa0_3$ AND $LiNb0_3$.**

r_{ij} (pm/V), n, ε_r	r_{13}	r_{33}	r_{51}	r_{22}	n_0	n_e	ε_{r0}	ε_{re}
$LiTa0_3$	7.5	33	20	1.0	2.176	2.180	41	43
$LiNb0_3$	8.6	30.8	28	3.4	2.286	2.200	43	28

Only the intersection of the refractive index ellipsoid and the plane transverse to the optical beam is of interest. That is to say, for the X-cut crystal, the index ellipse will be formed of the four bottom right coefficients of the tensor of Eq. (5). An electric field hardly rotates the optical axes of the crystal (because of the difference between n_0 and n_e) and a beam linearly polarized along the Z direction has its optical length L modified only by the field along the extraordinary axis E_z according to

$$L = n\,t = \left(n_e - \frac{1}{2} n_e^3\; r_{33}\; E_z \right) t\,, \tag{6}$$

with t the thickness of the crystal. The amplitude EW_r of a laser beam reflected by such a crystal is the sum of waves reflected by the first mirror or multiply reflected by the second mirror. It is given by

$$EW_r = EW_i \left(\rho_1 + t_1 t_1^c \rho_2^c e^{j\frac{4\pi L}{\lambda}} \sum_{n=0}^{\infty} (\rho_1^c \rho_2^c e^{j\frac{4\pi L}{\lambda}})^n \right), \tag{7}$$

with EW_i the incident amplitude, with ρ and t the reflection and the transmission coefficients, with indices *1* and *2* for the first and the second mirrors and superscript c for waves coming from the crystal, and with λ the wavelength in a vacuum. The total power reflection coefficient R is thus

$$R = \left| \rho_1 + \frac{(1-\rho_1^2)\rho_2^c e^{j\frac{4\pi L}{\lambda}}}{1 + \rho_1 \rho_2^c e^{j\frac{4\pi L}{\lambda}}} \right|^2 . \tag{8}$$

Fig. 2 shows reflection coefficient R versus wavelength for different values of the reflectance of the dielectric mirrors (same mirrors on both sides). An electric RF field will modulate length L, thus leading to a modulation of R proportional to the slope of the curves. One can see that a trade-off has to be achieved between the sensitivity of the probe and the possible range of the operating point.

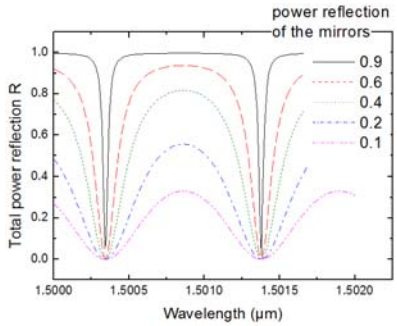

FIG. 2. Power reflection coefficient as a function of the reflection coefficient of the mirrors.

The sensitivity S_R of the reflectance versus electric field E_z is

$$S_R = \frac{\partial R}{\partial E_z} = 2R_0 \cdot \left| \mathrm{Re}\,al\left(\frac{j2\pi\, n_e^3 r_{33} t\,(1-\rho_1^2)\rho_2^c e^{j\frac{4\pi L_0}{\lambda}}}{\lambda\left(1+\rho_1\rho_2^c e^{j\frac{4\pi L_0}{\lambda}}\right)\left(\rho_1+\rho_2^c e^{j\frac{4\pi L_0}{\lambda}}\right)} \right) \right|, \tag{9}$$

where subscript 0 indicates a quantity without electric field applied, and where Real() denotes the real part of the complex number.

The EO signal V_{EO} measured by the spectrum analyzer at frequency ($f_e - f_0$) is proportional to the amplitude of the electric field:

$$V_{EO} = S_V\, E_z = C\,10^{\alpha/10}\, I\, Z_0\, S_R\, E_z, \tag{10}$$

with S_V the sensitivity of the probe [V/(V/m)], C the responsivity of the photodiode [A/W], α the losses [dB], I the modulated laser beam power [W], and $Z_0 = 50\Omega$. In our set-up, C = 0.95 A/W, I ~ 65mW, and α is estimated to be -6 dB without the optical switch and -7 dB with it.

Fig. 3 show the reflected light beam intensity (at frequency f_0) detected by the photodiode and the EO signal V_{EO} (at frequency f_e - f_0) as a function of the wavelength detuning Δλ, for both probes. The reference wavelength is 1.55 μm. These measurements were made without the optical switch and inside the TEM cell with an electric field of approximately 5 V/m inside the crystal. As predicted, the EO signal is proportional to the slope of the reflection curve. The differences between the two probes are attributed to the gluing of the EO crystals to the graded

index lenses, which modifies the reflection coefficient of the first mirror and in particular the shape of the curve (cf. Fig. 2 for different shapes according to the reflection coefficient of the mirrors). The best sensitivity for probe 2 is about 40 nV for 1 V/m in the crystal and that for probe 1 is about half this value. These numbers are in good agreement with theory (considering the reflectance curves). They could be far greater with good dielectric mirrors but it would then be difficult to use several probes with the same laser, because of the need to guaranty a precise crystal thickness. With a fixed operating point, the smallest measurable electric field will then principally depend on the quality of the spectrum analyzer. With an Agilent MXA N9020A model, the noise threshold is about -150dBm (7 nV) with 1 Hz bandwidth.

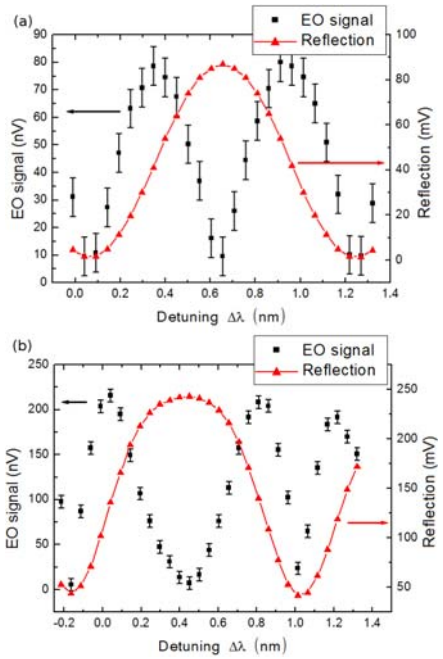

FIG. 3. EO signal and reflection for probe 1 (a) and probe 2 (b). Reference for λ is 1.55 μm.

Fig. 4 shows the measured EO signal when the two probes are used sequentially thanks to the optical switch. The position inside the TEM cell is not exactly the same as before, which explains the difference in the maxima of the signals. A sensitivity S_V of 14 nV(V/m) enables to have a signal equal to twice the noise threshold (7 nV) of the spectrum analyzer when measuring an electric field of 1 V/m in the crystal. With this limit for the two probes, a range of nearly 2 nm is possible for Δλ. This corresponds to a tuning range of nearly 2°C for the laser temperature.

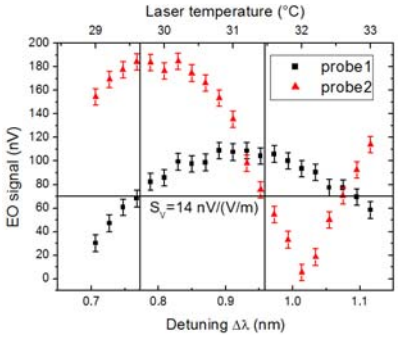

FIG. 4. EO signal for probe 1 (squared dots) and probe 2 (triangular dots) using the optical switch.

The best operating point, and therefore the best sensitivities for the probes, will depend on the experimental conditions (the temperature of the crystals being the most important parameter). To solve this issue, one solution is to use another RF emitting antenna (at another frequency f_{ref}) whose electric field at the different probe positions is well known. The probes will measure the RF field of the reference antenna at f_{ref} to estimate their sensitivities, and measure at the same time the device under test at its own frequency. The laser wavelength can also be tuned antenna to ensure maximum sensitivity, thanks to the known sensitivity obtained with the reference antenna.

Other measurements were performed with a 30 dB power amplifier at f_e = 1.8 GHz, allowing to obtain a stronger electric field in air and inside the phantom liquid. Fig. 5 shows the EO signal (in dBm) in air and inside the liquid according to the external electric field (and no longer the field inside the EO crystal). As predicted, the slope of the curves is 20dB per decade. This means that the photodiode output current is proportional to the external field. The sensitivity S_{ext} of the probe is better inside the liquid (26 nV for an external field of 1 V/m) than in air (3.7 nV/(V/m)). This is a consequence of the electric field inside the crystal being lower than in air, because of the high permittivity of the EO crystal. Since the permittivities of the EO crystal and of the liquid are nearly the same, however, electric fields inside the crystal and inside the liquid are similar. Simulations with CST Microwave showed that the field inside the EO crystal is about 4 times lower than in air. When the probe is inside the liquid, the graded index lens concentrates the optical beam and leads to an increase inside the crystal of about 15%. Being in the liquid, the second mirror properties are changed, leading to a small change in the reflectance curve (cf. fig. 6) and therefore to a small change in the maximum sensitivity.

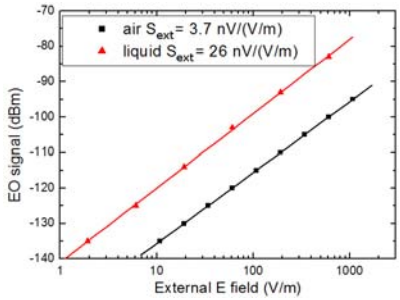

FIG. 5. EO signal in air and in the liquid vs the external E field.

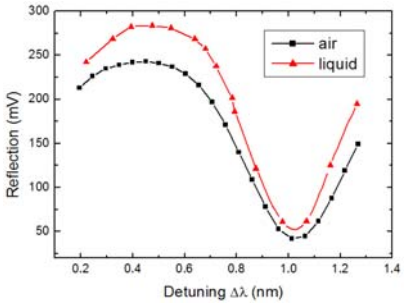

FIG. 6. Reflection in air and liquid.

The probe was also rotated manually to align the electric field along other directions. The detected EO signal was very weak and comparable in magnitude to the positioning imprecision.

As a conclusion, we have proposed a way to measure the SAR of mobile phones using a matrix of EO sensors. Electro-optic probes were specifically designed for this application. The technique is akin to the Fabry-Perot resonator technique, but uses low-reflectivity dielectric mirrors. In both cases, a modification of the optical length by the electric field leads to a variation in the reflection signal. Low-reflectivity mirrors, however, decrease the sensitivity of the probes but enable us to use a single laser for the addressing of all probes. A heterodyne system with two EO probes interrogated by a single laser was built as a proof-of-concept. The detection limit of the electric field inside the crystal or inside the phantom liquid is better than 1 V/m. An auto calibration technique and the adjustment of the laser wavelength using a reference antenna were also proposed. In order to measure a longitudinal electric field instead of a transverse one, an isotropic EO crystal can be used with the same set-up. The laser must be linearly polarized along one of the optical axes, i.e., tilted by an angle of $\pi/4$ away from crystallographic axes.

The authors would like to acknowledge fruitful discussions with Bernard Cretin and Vincent Laude. This work was supported by French National Agency (ANR) under project MERODAS ANR-08-VERSO-011.

[1]ICNIRP, "Guidelines for limiting exposure to time-varying electric, magnetic, and electromagnetic fields (up to 300 GHz)," Health Phys., vol. 74, no. 4, pp. 494–522, ICNIRP Guidelines, Apr. 1998

[2]IEEE standards for safety levels with respect to human exposure to radio frequency electromagnetic fields 3 KHz to 300 GHz, IEEE Standard C95.1, 1991.

[3]The Council of the European Union "council recommendation of 12 July 1999 on the limitation of exposure of the general public to electromagnetic fields (0 Hz to 300 GHz)" Official Journal of the European Communities, L 199/59, 1999/519/CE, July 1999.

[4]Basic Standard for the Measurement of Specific Absorption Rate Related to Exposure to Electromagnetic Fields from Mobile Phones (300 MHz–3 GHz), EN 50361, 2001.

[5]H. I. Bassen, *19th international Conference - IEEE/EMBS*, Chicago, IL. USA Oct. 30 - Nov. 2, 1997, pp. 2492-2495.

[6]Q. Chen, M. Tani, Zhiping Jiang, and X.-C. Zhang, J. Opt. Soc. Am. B 18, 823 (2001).

[7]L. Duvillaret, S. Rialland and J.-L. Coutaz, J. Opt. Soc. Am. B 19, 2692 (2002).

[8]L. Duvillaret, S. Rialland and J.-L. Coutaz, J. Opt. Soc. Am. B19, 2704 (2002).

[9]H. Togo, A. Sasaki, A. Hirata,T. Nagatsuma, Int. J. of RF and Microwave Computer-Aided Engineering 14, 290 (2004).

[10]H. Togo, N. Shimizu and T. Nagatsuma, IEICE Trans. Electron. E90-C, 436 (2007).

[11]H. Togo, N. Kukutsu, N. Shimizu and T. Nagatsuma, J. Lightwave Tech. 26, 2700 (2008).

[12]M. Bernier, L. Duvillaret, G. Gaborit, A. Paupert, and J.-L. Lasserre, IEEE Sensors J. 9, 61 (2009).

[13]D.-J. Lee, N.-W. Kang, J.-H. Choi, J. Kim and J. F. Whitaker, Sensors 11, 806 (2011).

[14]B.E.A. Saleh, M.C. Teich, *Fundamentals of Photonics* (Wiley Series in Pure and Applied optics, second edition, Hoboken New Jersey 2007), p. 851.

[15]S. Zhang, S. Euphrasie, P. Vairac and B. Cretin, *5th International Conference on electromagnetic Near-field (NF) Characterization and Imaging ICONIC 2011*, Rouen, France, 30 November–2 December 2011, pp. 3A.

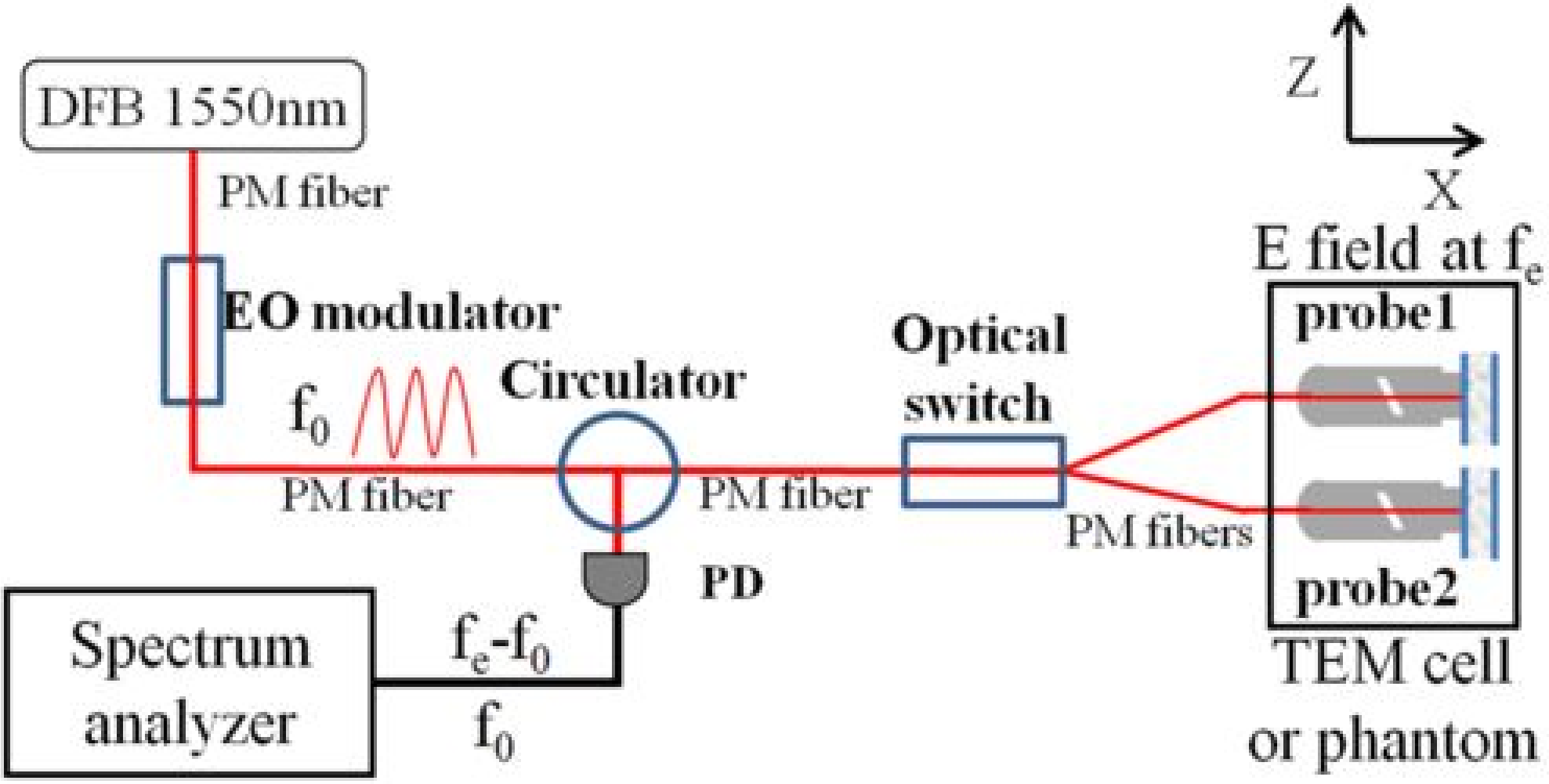
DFB 1550nm
PM fiber
EO modulator
f_0
Circulator
PM fiber
PM fiber
Optical switch
PM fibers
PD
Spectrum analyzer
f_e-f_0
f_0
Z
X
E field at f_e
probe1
probe2
TEM cell or phantom

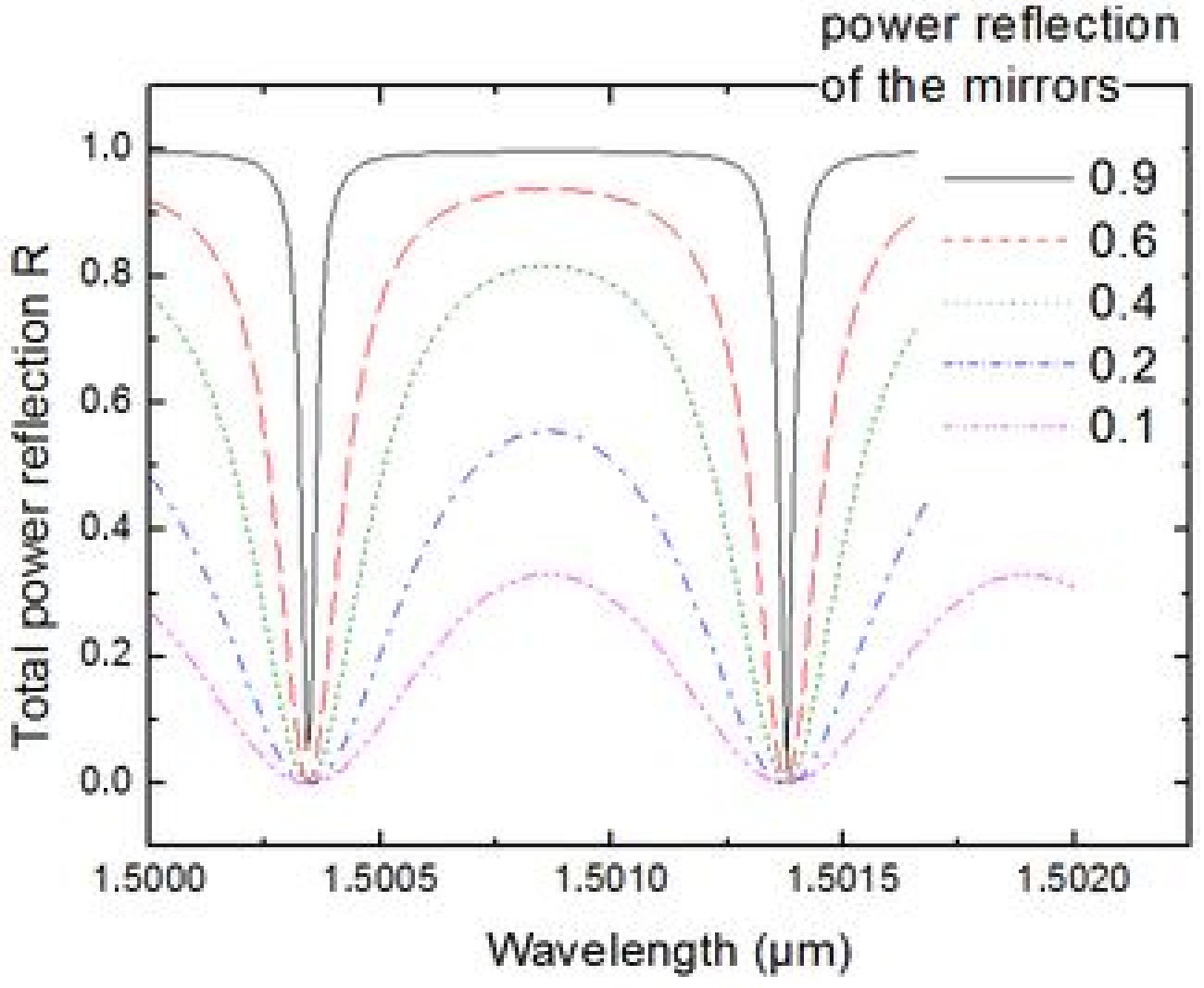
power reflection
of the mirrors
0.9
0.6
0.4
0.2
0.1
Total power reflection R
1.0
0.8
0.6
0.4
0.2
0.0
1.5000
1.5005
1.5010
1.5015
1.5020
Wavelength (μm)

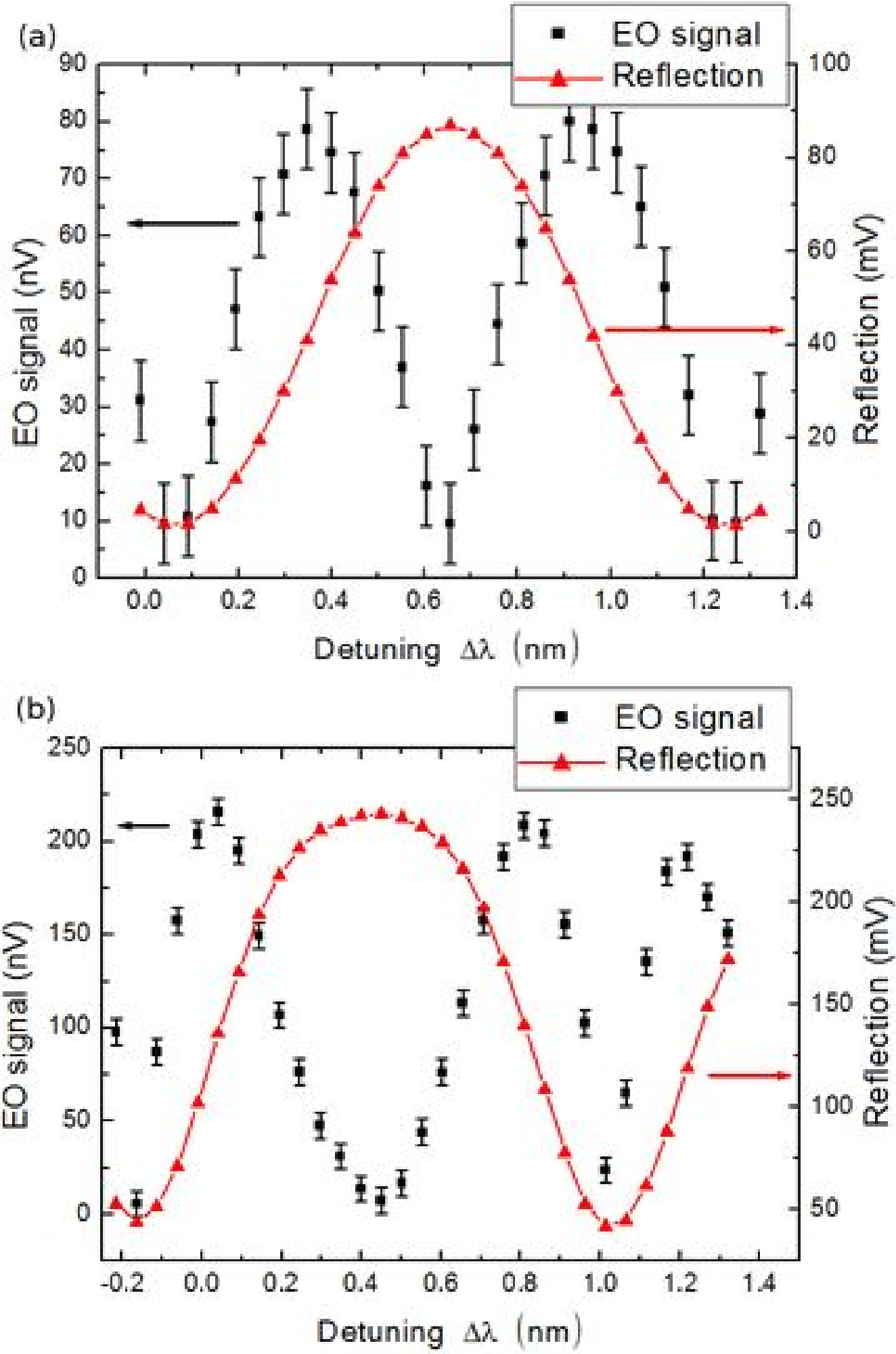
(a)
EO signal
Reflection
EO signal (nV)
Reflection (mV)
Detuning Δλ (nm)
(b)
EO signal
Reflection
EO signal (nV)
Reflection (mV)
Detuning Δλ (nm)

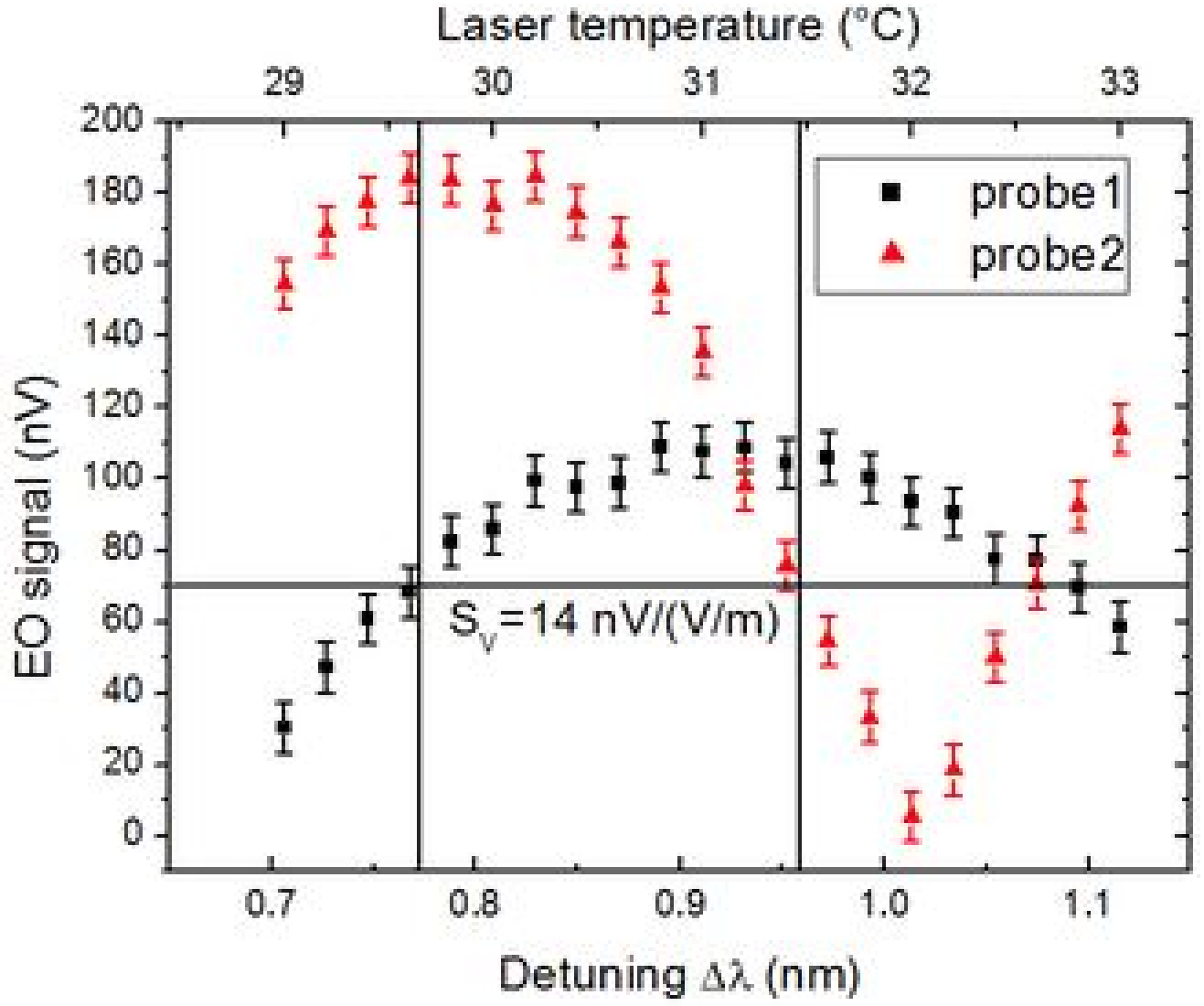
Laser temperature (°C)
29
30
31
32
33
200
180
160
140
120
100
80
60
40
20
0
EO signal (nV)
probe1
probe2
S_V=14 nV/(V/m)
0.7
0.8
0.9
1.0
1.1
Detuning Δλ (nm)

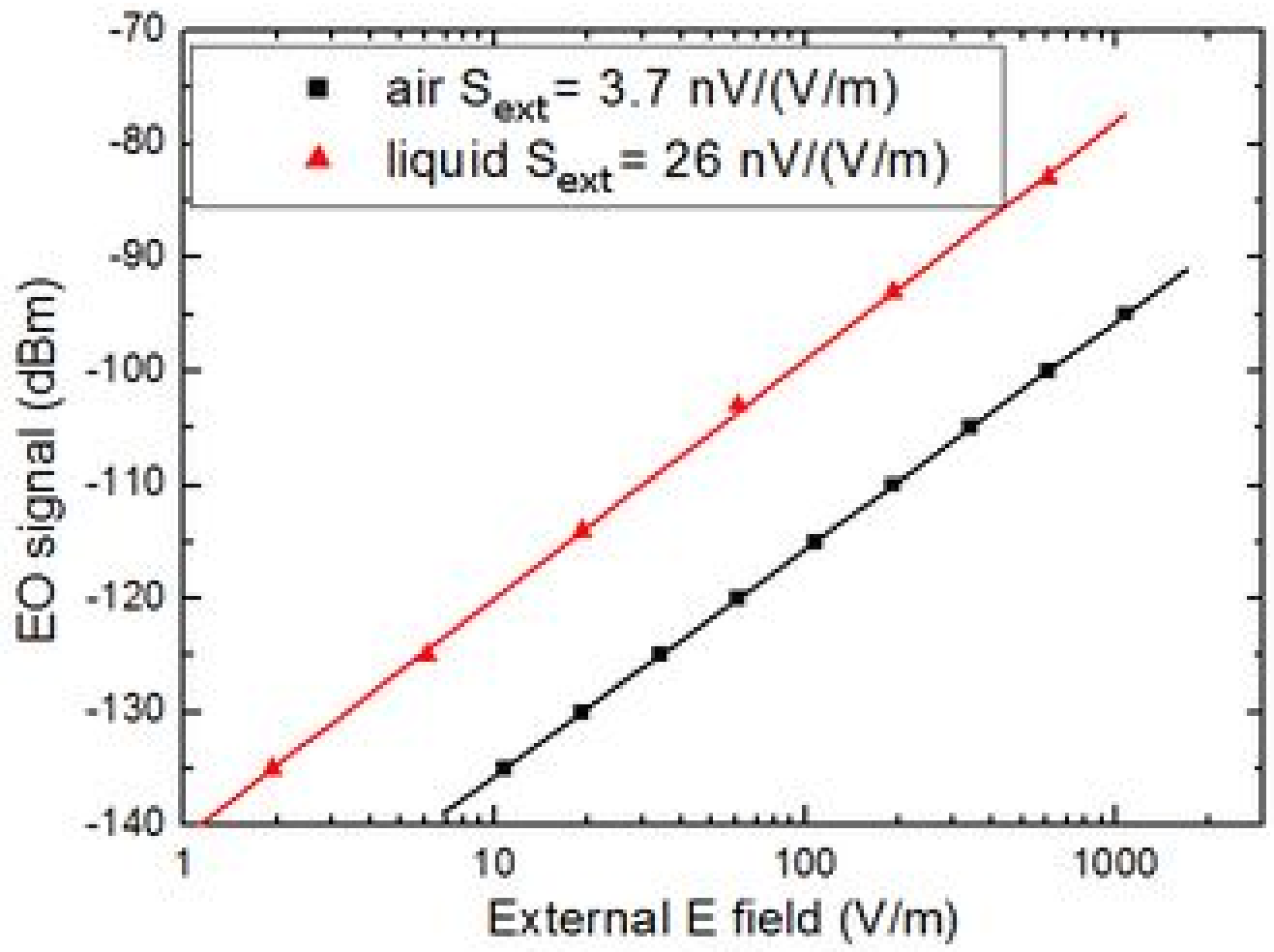
air S_{ext}= 3.7 nV/(V/m)
liquid S_{ext}= 26 nV/(V/m)
EO signal (dBm)
-70
-80
-90
-100
-110
-120
-130
-140
1
10
100
1000
External E field (V/m)

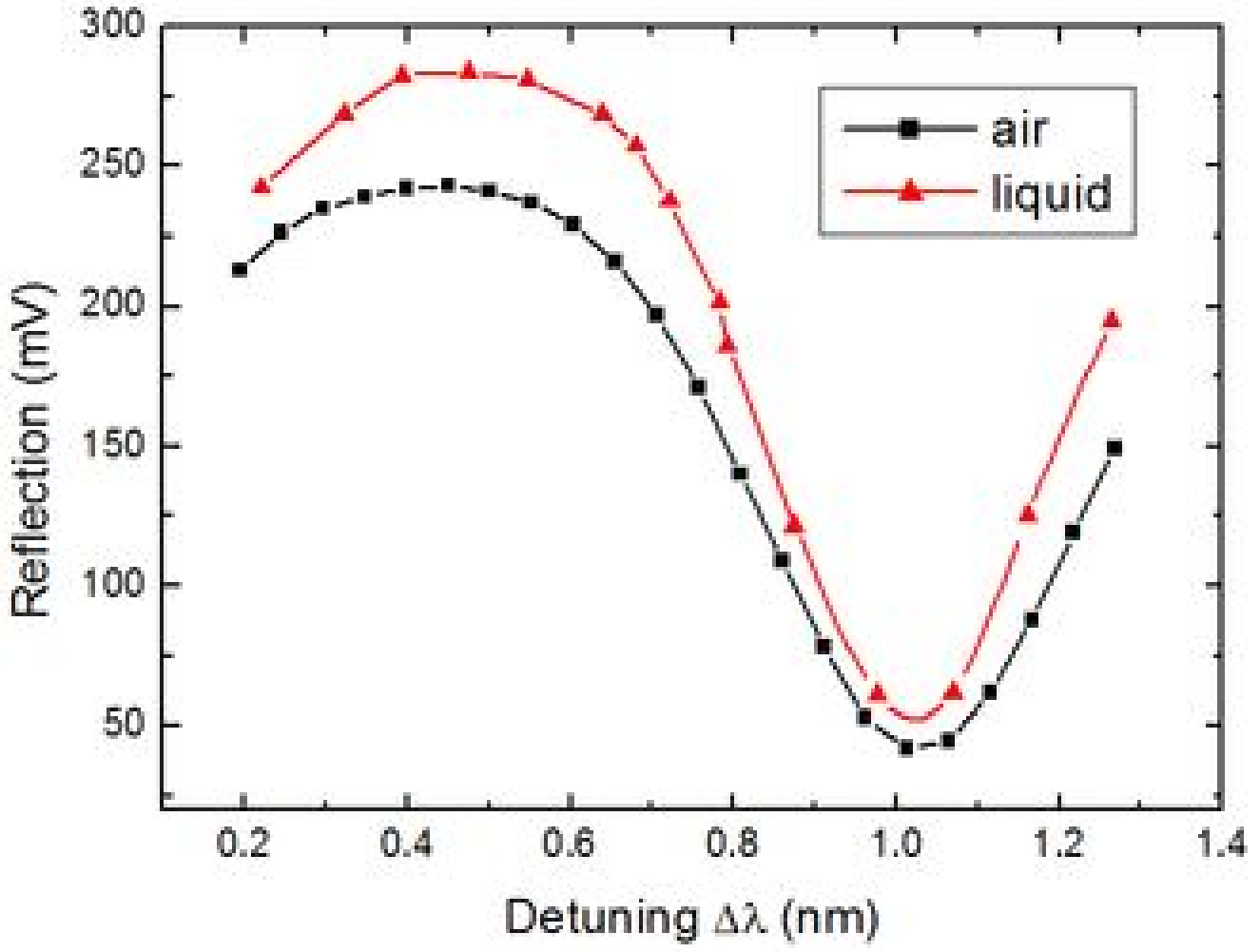
300
250
200
150
100
50
Reflection (mV)
0.2
0.4
0.6
0.8
1.0
1.2
1.4
Detuning Δλ (nm)
air
liquid